# Fabrication and Photoconductivity Study of Copper Phthalocyanine/Perylene Composite with Bulk Heterojunctions Obtained by Solution Blending

**Xiong Mo, Hong-Zheng Chen,* Yong Wang, Min-Min Shi, and Mang Wang**

*Department of Polymer Science and Engineering, State Key Lab of Silicon Materials, Zhejiang University, Hangzhou 310027, People's Republic of China*

*Received: January 22, 2005; In Final Form: March 3, 2005*

Copper tetra-(octyl-alkoxy-carbonyl)-phthalocyanine (CuPc-C8) and 3,4,9,10-tetra-(octyl-alkoxy-carbonyl)-perylene (Pery-C8) attached with long alkyl chains by covalent bonds were synthesized. Both of the two compounds showed good solubility in organic solvents, and the compatibility between them was improved. The novel composite of CuPc-C8/Pery-C8 was prepared by the solution-blending method. Atomic force microscopy (AFM) demonstrated the formation of the bulk heterojunction structure in their cast-coated films. Enhanced photosensitivity was observed in the photoreceptor made from the CuPc-C8/Pery-C8 composite, which was interpreted in terms of the large interfacial area between the two components due to the existence of the bulk heterojunction structure.

## Introduction

Recently, many scientists have shown great interest in the new concept of "bulk heterojunctions", which has been introduced to describe organic photovoltaic (OPV) devices.[1−3] The progress in OPV is chiefly attributed to the introduction of the donor−acceptor heterojunction that functions as a dissociation site for the strongly bound photogenerated excitons.[4,5] Further progress was realized by using blends of the donor and acceptor materials.[6,7] It was found that phase separation during spin-coating led to a bulk heterojunction that removed the exciton diffusion bottleneck by creating an interpenetrating network of the donor and acceptor materials. Such blends allow some efficiency in the fundamental steps necessary to achieve significant solar cell efficiency, which include absorption of light, creation and separation of carriers at the donor/acceptor (D/A) interfaces, and transport of the carriers through the bulk of the device from the creation site to the appropriate collecting electrodes. Phthalocyanine (Pc) and perylene (Pery) are typical electron donor and acceptor materials, respectively. A number of OPV cells based on them have been investigated.[8−11] However, due to their poor solubility, the "bulk heterojunction" based on them was obtained mostly by the co-deposition method, which is costly and inconvenient.

In this paper, we demonstrated a simple method to fabricate the D/A composite with bulk heterojunctions from soluble copper phthalocyanine (CuPc) and perylene (Pery) derivatives as the electron donor and electron acceptor, respectively. The molecular structures of the two compounds are shown in Figure 1. The bulk heterojunction and photoconductivity of copper tetra-(octyl-alkoxy-carbonyl)-phthalocyanine (CuPc-C8)/3,4,9,10-tetra-(octyl-alkoxy-carbonyl)-perylene (Pery-C8) composites in cast-coated films were investigated as well.

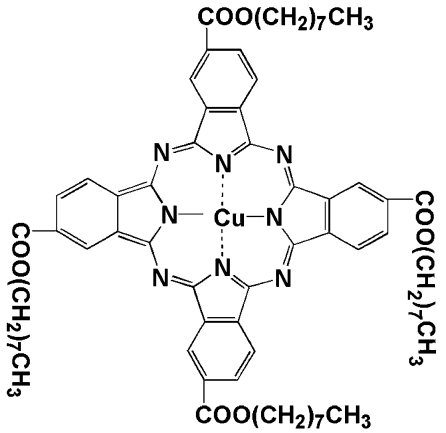


**Figure 1.** Chemical structures of CuPc-C8 and Pery-C8.

## Experimental Section

Perylene-3,4,9,10-tetracarboxylicdianhydride (PTCDA), copper tetra-carboxyl-phthalocyanine ($CuPc(COOH)_4$), polycarbonate (PC), and *N*,*N*′-diethyl-4-aminobenzaldehyde-1-pheny-(α-naphthyl)-hydrazone (BAH) were commercially available and used without further purification. All solvents used were analytical grade and were distilled before use.

A $^1H$ NMR spectrum was taken on an Avance 500 MHz spectrometer. The contents of C, H, and N were measured on a Perkin-Elmer 2400C element analysis apparatus. The emission spectrum was recorded on a Hitachi F-4500 fluorescence spectrophotometer, and UV−vis absorption was recorded by a Cary Bio100 spectrophotometer. The cyclic voltammogram (CV) was taken by a CHI660 electrochemistry workstation. Film thickness was measured on an Elektko-Physik minitest 2000

* Author to whom correspondence should be addressed. Phone: +86-571-87952557. Fax: +86-571-87951635. E-mail: hzchen@zju.edu.cn.

10.1021/jp050391+ CCC: $30.25 
Published on Web 03/29/2005

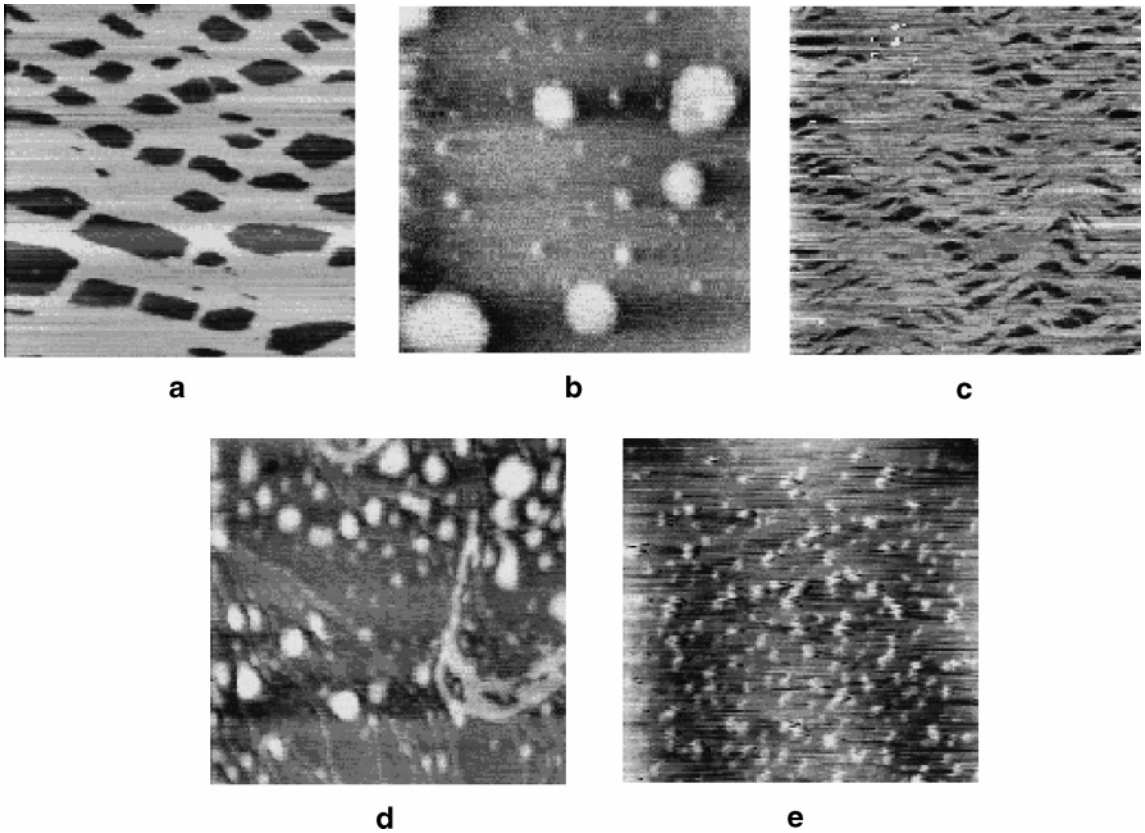


**Figure 2.** AFM images of cast films 2 $\mu$m × 2 $\mu$m on mica corresponding to (a) CuPc-C8, (b) Pery-C8, (c) CuPc-C8/Pery-C8 (80:20 molar ratio), (d) CuPc-C8/Pery-C8 (50:50 molar ratio), and (e) CuPc-C8/Pery-C8 (20:80 molar ratio).

thin film measuring apparatus. The morphology of the films was observed by atomic force microscopy (AFM) SPA400 + SPI3800. X-ray diffraction patterns were obtailed at Pigaku D/Max-38.

CuPc-C8 was synthesized by esterification of $CuPc(COOH)_4$ with octanol and purified by precipitation in acetone.[12] $^1$H NMR-(500 MHz/$CDCl_3$): $\delta$ (ppm vs TMS) 8.69−7.60 (12H from the CuPc ring), 3.85 (8H from $-O-CH_2-$), 1.67−1.30 (48H from $-(CH_2)_6-$), 0.90 (12H from $-CH_3$). Anal. Calcd. for CuPc-C8 ($C_{69}H_{83}CuN_8O_8$): C, 68.15; H, 6.88; N, 9.21. Found: C, 67.95; H, 6.98; N, 9.53. Pery-C8 was synthesized by esterification of PTCDA with octanol and was chromatographically purified.[13] $^1$H NMR (500 MHz/$CDCl_3$): $\delta$ (ppm vs TMS) 8.08−7.92 (8H from the perylene ring), 4.33(8H from $-O-CH_2-$), 1.81−1.35 (48H from $-(CH_2)_6-$), 0.91(12H from $-CH_3$). Anal. Calcd. for Pery-C8 ($C_{56}H_{76}O_8$): C, 76.68; H, 8.73. Found: C, 76.46; H, 8.92.

The CuPc-C8/Pery-C8 composite was obtained by mixing the $CHCl_3$ solutions containing the two components, respectively. If not noted, the proportions between the two components are molar ratios. The composite films were prepared by the cast-coating method.

The photoconductivity of CuPc-C8/Pery-C8 composites was studied in dual-layer photoreceptors. The photoreceptor was composed of the charge generation layer (CGL) and the charge transportation layer (CTL) on an aluminum substrate. The CGL was formed to 1 $\mu$m thickness from the $CHCl_3$ solution containing Pery-C8 or CuPc-C8 and their mixture. The CTL consisted of 50 wt % *N*,*N*-diethyl-4-aminobenzaldehyde-1-pheny-(α-naphthyl)-hydrazone (BAH) in polycarbonate (PC) matrix, and the thickness was 25 $\mu$m.[14]

Photoconductivity measurements were carried out on a GDT-II model photoconductivity-measuring device by the photoinduced xerographic discharge technique.[15] The intensity of exposure light ($I$) was set at 1.1 mJ/cm$^2$ during measurement, where a halogen lamp (5 W, 24 V) was used as light source. In the measurement, the surface of the dual-layer photoreceptor was negatively charged in the dark with initial surface potential ($V_0$). The photoinduced discharge curve was recorded by a computer, from which $V_0$, residual potential ($V_r$), and time from original surface potential to half under illumination ($t_{1/2}$) can be obtained. The photosensitivity was characterized by the half-decay exposure energy ($E_{1/2}$), which is defined as the product of the half-decay time ($t_{1/2}$) and the intensity of exposure light ($I$), i.e., $E_{1/2} = It_{1/2}$. A desired photoreceptor should have a large $V_0$, a small $V_r$, and $t_{1/2}$. The smaller the $E_{1/2}$, the higher the photosensitivity of the photoreceptor.

## Results and Discussion

**Morphology of the Cast-Coated Film.** The evolution of the surface morphology of the cast films from the blended solutions containing different contents of CuPc-C8 and Pery-C8 can be observed by AFM as shown in Figure 2. The pristine CuPc-C8 film appears to have a quite regular grid structure with some apertures in a homogeneous matrix (Figure 2a), while the pure Pery-C8 has a poor film-forming characteristic, and asymmetric size grains are distributed randomly in the film (Figure 2b). After they are blended, the film morphology of the composite is quite different. The film of the CuPc-C8/Pery-C8 composite with the 80:20 molar ratio appears more compact than the film of pure CuPc-C8, and the sizes of the apertures in the film are smaller as well (Figure 2c). When the proportion of the composite is 50:50, the phase separation appears, and the film is composed of grains and fibers adhering closely (Figure 2d). The interesting thing is that small and uniform grains are found in the composite film by increasing the content of Pery-C8 to

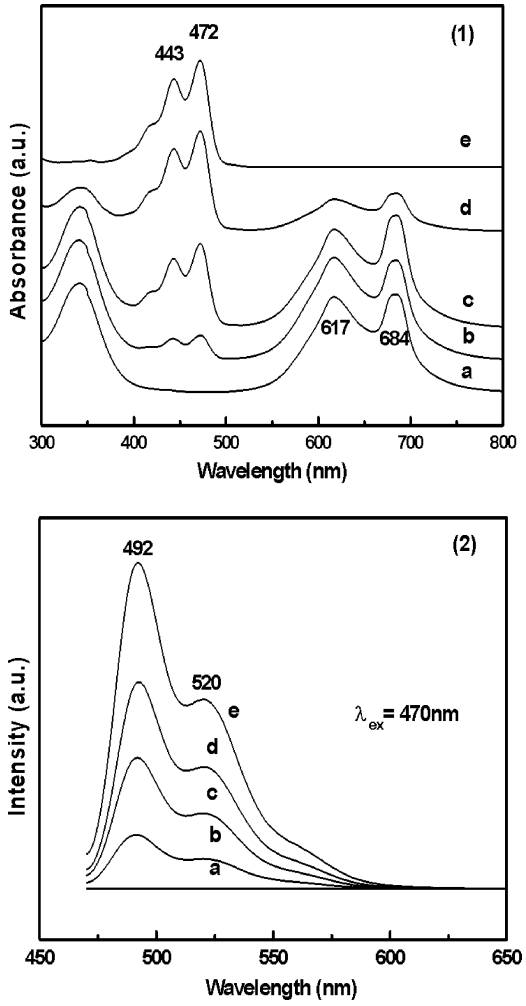


**Figure 3.** (1) UV−vis absorption and (2) fluorescence spectra of (a) CuPc-C8, (b) CuPc-C8/Pery-C8 (80:20 molar ratio), (c) CuPc-C8/Pery-C8 (50:50 molar ratio), (d) CuPc-C8/Pery-C8 (20:80 molar ratio), and (e) Pery-C8 in $CHCl_3$ ($C = 1 \times 10^{-5}$ mol/L); the excitation wavelength is 470 nm.

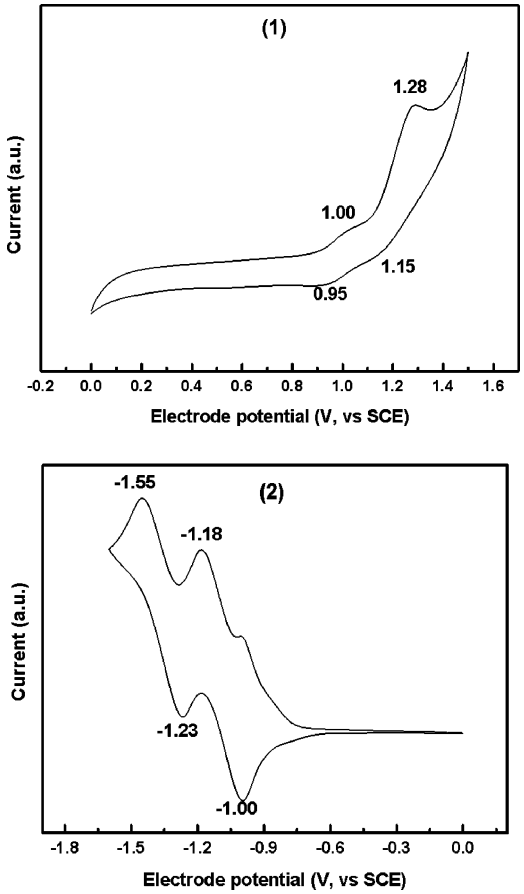


**Figure 4.** CV for (1) CuPc-C8 and (2) Pery-C8 in a 0.1 mol/L $TBAPF_6$/$CHCl_3$ solution with a SCE as reference and a Pt counter electrode at scan rate of 50 mV/s.

80% by the molar ratio (Figure 2e). Such evolution of the film morphology suggests that there might exist a bulk heterojunction in the CuPc-C8/Pery-C8 composite in suitable proportion.[16] It can be explained that during cast-coating and solvent evaporation the phase separation is induced by the interaction of CuPc-C8 and Pery-C8 molecules, creating an intricate interpenetrating network. It is expected that, after photon absorption and exciton creation, the exciton should be dissociated at the large D/A interfacial area created by the blend structure, which is favorable to the dissociation of excitons and is promising for use in organic optoelectronic devices.

**Absorption, Emission, and Electrochemical Characteristics in Solution.** Absorption and emission spectra of CuPc-C8, Pery-C8, and their blends in chloroform ($CHCl_3$) are shown in Figure 3. CuPc-C8 shows two peaks of the Q-band at 617 and 684 nm, representing the characteristic bands of the dimer and the monomer of CuPc, respectively,[17] besides a peak of the Soret band at 340 nm. The spectrum of Pery-C8 shows a vibronic structure with two peaks at 443 and 472 nm with one shoulder, and the absorption bands are reminiscent of those of pure perylene, the dipole moment of which is directed parallel to the long axis of the molecule.[18,19] The spectra of CuPc-C8/Pery-C8 composites in $CHCl_3$ are the superposition of their respective absorption spectra, and the relative intensity of the peaks corresponding to these two compounds changes with the relative content in the composite, indicating the absence of significant electronic interaction between CuPc-C8 and Pery-C8 in solution. The emission spectrum of Pery-C8 shows peaks at 492 and 512 nm, and CuPc-C8 has no fluorescence in $CHCl_3$ solution. It was found that the emission spectra of the CuPc-C8/Pery-C8 composite only exhibits the characteristic emission of pure Pery-C8, the intensity of which decreases consistently with the increasing content of CuPc-C8 in the composite, suggesting no charge and energy transfer in the ground state between the two compounds.

Figure 4 shows the CV for CuPc-C8 and Pery-C8 in a 0.1 mol/L $TBAPF_6$/$CHCl_3$ solution with a saturated calomel electrode (SCE) as the reference and Pt as the counter electrode. It was found that CuPc-C8 has two pairs of redox peaks at 1.00/0.95 and 1.28/1.15 V vs SCE, and Pery-C8 has two pairs of redox peaks at −1.18/−1.00 and −1.55/−1.23 V vs SCE. From the first oxidation peak (1.00 V vs SCE) of CuPc-C8 and the first reduction peak (−1.00 V vs SCE) of Pery-C8, the highest occupied molecular orbital (HOMO) of CuPc-C8 and the lowest unoccupied molecular orbital (LUMO) of Pery-C8 can be estimated as −5.60 and −3.60 eV vs the vacuum level, respectively, taking −4.6 eV as SCE vs the vacuum level. The optical band gap of CuPc-C8 and Pery-C8 can be obtained from their absorption spectra to be ca. 1.72 and 2.48 eV, respectively. So the LUMO of CuPc-C8 and the HOMO of Pery-C8 are calculated to be ca. −3.88 and −6.08 eV vs the vacuum level, respectively. The obtained energy level data will be discussed later in the paper.

**Absorption Spectra and X-ray Diffraction Patterns of Cast-Coated Films.** Absorption spectra and X-ray diffraction patterns of the cast-coated films of CuPc-C8, Pery-C8, and their

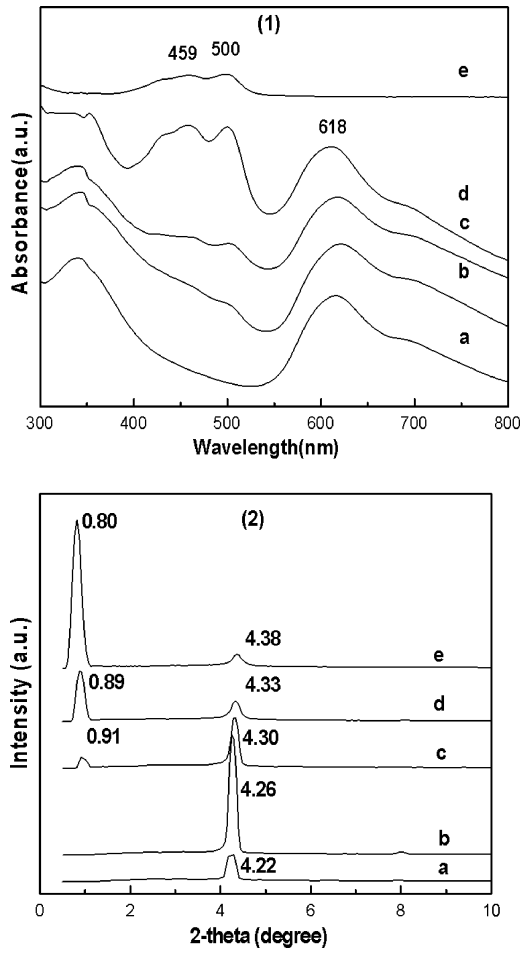


**Figure 5.** (1) UV−vis absorption spectra and (2) X-ray diffraction patterns of (a) CuPc-C8, (b) CuPc-C8/Pery-C8 (80:20 molar ratio), (c) CuPc-C8/Pery-C8 (50:50 molar ratio), (d) CuPc-C8/Pery-C8 (20:80 molar ratio), and (e) Pery-C8 cast-coated films.

blends are shown in Figure 5. In comparison to their absorption in $CHCl_3$ solution (as shown in Figure 3, part 1), the absorption peaks of pure CuPc-C8 and Pery-C8 films become red-shifted and broader due to the aggregation of CuPc-C8 and Pery-C8 molecules. The absorption spectra of the CuPc-C8/Pery-C8 films change with the variation in the relative content of these two compounds. The relative intensities of the peaks corresponding to these two compounds change with the relative content in the composite, the same as that in solution. However, the Q-band centered at 616 nm of CuPc-C8 tends to be blue-shifted with increasing content of Pery-C8 in the composite films, due to the size decrease of the CuPc-C8 grains in the composite film.

The X-ray diffraction patterns of cast-coated films are shown in Figure 5, part 2. It was found that the pure CuPc-C8 film has a single peak at 4.22° (plot a), corresponding to an interplanar spacing of 20.91 Å, implying a crystal structure of oriented parallel planes. The pure Pery-C8 film has a main sharp peak at 0.80° (plot e). In the case of the CuPc-C8/Pery-C8 (80:20 molar ratio) composite film, the intensity of the diffractive peak corresponding to CuPc-C8 increases greatly (plot b). When the blending proportion is 50:50, the intensity of the peak becomes weak, and a new peak appears at 0.91° (plot c). When the blending proportion is 20:80 for CuPc-C8/Pery-C8, the relative intensity of the peaks at 4.33° and 0.89° reverses (plot d) compared to the composite with the 50:50 molar ratio.

All of these changes in the UV−vis absorption spectra and X-ray diffraction patterns of the composite films might stem from the changes in the aggregation structure of the CuPc-C8 and Pery-C8 molecules with the variation of relative content. When the content of Pery-C8 in the composite is increased, the phase separation appears gradually due to the interaction of CuPc-C8 and Pery-C8, corresponding to the two diffraction peaks appearing and the relative intensity changes. The diffraction angle of $2\theta$ corresponding to each component becomes bigger, indicating that the interplanar space of each component decreases in the film. It means that the more compact film could be obtained by increasing the content of Pery-C8 in the composite, which is consistent with AFM observation.

**TABLE 1: Photosensitive Parameters of CuPc-C8, Pery-C8, and Their Composites**[a]

| | $V_0$ (V) | $V_r$ (V) | $t_{1/2}$ (s) | $S$[b] ($mJ^{-1}$ $cm^2$) |
|---|---|---|---|---|
| CuPc-C8 | 867 | 267 | 3.67 | 0.24 |
| CuPc-C8/Pery-C8 (80:20 molar ratio) | 875 | 112 | 0.98 | 0.93 |
| CuPc-C8/Pery-C8 (50:50 molar ratio) | 812 | 93 | 0.70 | 1.30 |
| CuPc-C8/Pery-C8 (20:80 molar ratio) | 853 | 65 | 0.46 | 1.97 |
| Pery-C8 | 881 | 68 | 0.56 | 1.62 |

[a] $V_0$, initial surface potential; $V_r$, residual potential; $t_{1/2}$, half-decay time. [b] The photosensitivity $S = E_{1/2}^{-1}$ when exposed to white light.

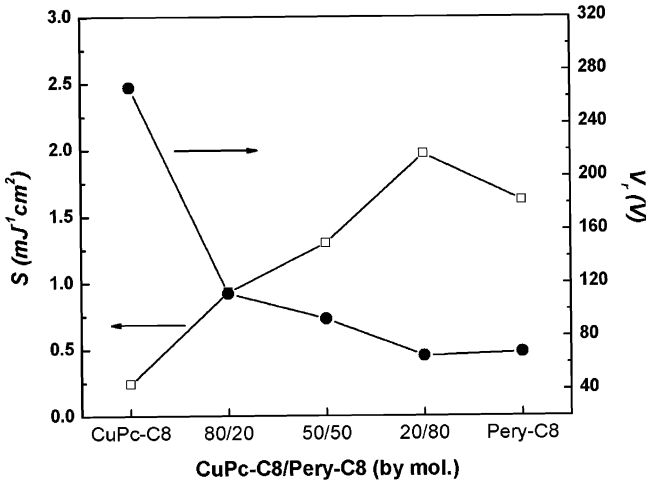


**Figure 6.** Photosensitivity ($S$) and residual potential ($V_r$) of CuPc-C8, Pery-C8, and their composites with different proportions when exposed to white light.

**Photoconductivity.** Table 1 presents the photoconductive properties of CuPc-C8, Pery-C8, and their blends. The changes in the photosensitivity ($S$) and residual potential ($V_r$) of CuPc-C8/Pery-C8 composites with different molar ratios of the two components is given in Figure 6. We can find that, under the same exposure conditions, the photoreceptor of pure CuPc-C8 shows a photosensitivity ($S$) of 0.24 $mJ^{-1}$ $cm^2$. After being blended with 20% Pery-C8, the photosensitivity increases to 0.93 $mJ^{-1}$ $cm^2$, 4-fold higher than that of pure CuPc-C8 and even better than that of the Pery-C8 film. It suggests that the cooperative interaction between the two molecules instead of the additive photosensitivity of the individual compounds is responsible for the improved photosensitivity. The photosensitivity of the composite increases further by increasing the content of Pery-C8 and reaches the highest at 1.97 $mJ^{-1}$ $cm^2$ when the content of Pery-C8 increases to 80%. It is also found that the residual potential ($V_r$) of these photoreceptors decreases gradually by increasing the content of Pery-C8 in the composite films and reaches the lowest at the same molar ratio of 20:80 between CuPc-C8 and Pery-C8, indicating the best photosensitivity for the composite with the mentioned ratio. The experiments were repeated for three times, and each time, three dual-layer photoreceptors were fabricated for every different mixing ratio

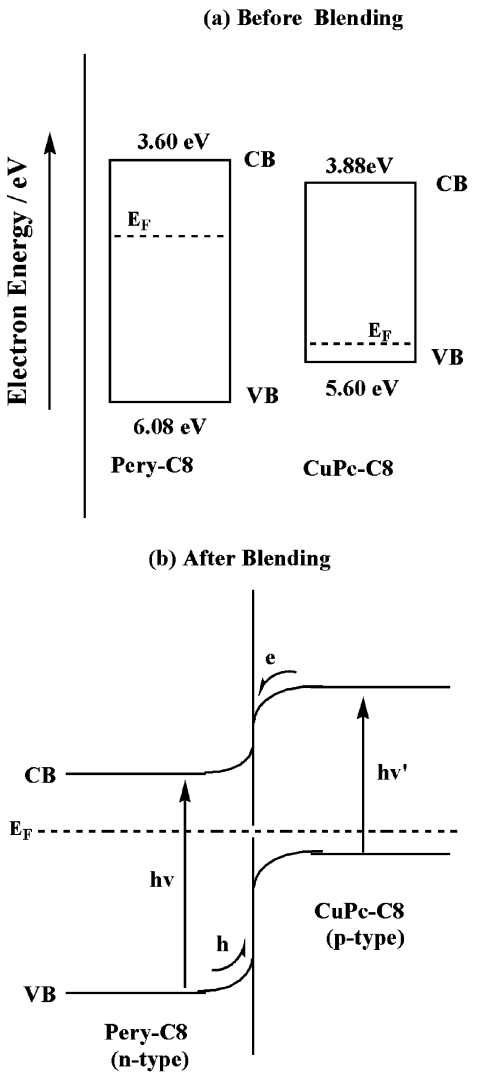


**Figure 7.** Energy band diagram of CuPc-C8 and Pery-C8 (a) before and (b) after blending. CB, VB, and $E_F$ denote the conduction band, valence band, and the Fermi level, respectively.

solution. The results showed reliably that the photoconductivity is the best when the molar mixing ratio of the CuPc-C8 and Pery-C8 is 20:80.

The substantial enhancement in photosensitivity achieved in the CuPc-C8/Pery-C8 composite is thought to result from the large interfacial area in the bulk heterojunction. As can be seen from AFM (Figure 2), the phase separation appears gradually in the composite film by increasing the content of Pery-C8, and the size of grains becomes the smallest when the content of Pery-C8 is raised to 80%, leading to the largest interfacial area between CuPc-C8 and Pery-C8 in the whole bulk of the film, corresponding to the best photoconductivity.

Figure 7 shows the energy band diagram of CuPc-C8 and Pery-C8 before and after blending. The HOMO and LUMO energy levels were calculated from the CV measurements and UV−vis spectra discussed in above. The Fermi levels are estimated according to ref 10. Because of the formation of p−n heterojunctions, a blend of energy bands occurs in the interface. The absorption of different wavelength light induces the creation of an exciton in both compounds; the interfaces between them act as the dissociation cites, where the photoinduced excitons split into free charge carriers. Increasing the heterojunction interface is favorable for the photoinduced excitons to split into free charge carriers.[20] Due to the existence of the interfacial potential barrier, as demonstrated by the built-in potential in the D/A heterojunction, it is difficult for the split electrons and holes to be close to each other, making it possible to leave holes in the donor phase of CuPc-C8 and electrons in the acceptor phase of Pery-C8. At the same time, the electrons and holes can be transported effectively in the Pery-C8 phase and CuPc-C8 phase to the Al substrate and the CTL, respectively, resulting in higher photosensitivity in the CuPc-C8/Pery-C8 composite.[21] The larger the interfacial area in p−n heterojunction, the higher the photosensitivity. In other words, it may help to remove the photogenerated electrons and holes out of the recombination ranges. Therefore, the early recombination of carriers is inhibited by the spatial separation of holes (on CuPc-C8) and electrons (on Pery-C8), which enhances the carrier lifetime, and subsequently improves the photoconductivity as well. Since the interfacial area of the CuPc-C8/Pery-C8 composite with the molar ratio of 20:80 is the largest, the best photoconductivity is observed in the composite.

## Conclusions

The solubility and compatibility of CuPc and perylene were improved greatly after being attached with long alkyl chain by covalent bonds, such that the CuPc-C8/Pery-C8 composites could be prepared by the solution-blending method. Due to the interaction of CuPc-C8 and Pery-C8 molecules, a bulk heterojunction structure could be formed in the composite film with a suitable content ratio, leading to the enhanced photosensitivity in the photoreceptor made from this composite. The results can help us to design photoconductive or photovoltaic devices with a high efficiency of charge carrier generation.

**Acknowledgment.** This work was financed by the National Natural Science Foundation of China (Grant Nos. 50225312 and 50433020).

## References and Notes

(1) Sariciftci, N. S.; Smilowitz, L.; Heeger, A. J.; Wuld, F. *Science* **1992**, *258*, 1474.
(2) Yu, G.; Gao, J.; Hummeler, J. C.; Wuld, F.; Heeger, A. *Science* **1995**, *270*, 1789.
(3) Vangeneugden, D. L.; Vanderzande, D. J. M.; Salbeck, J.; van Hal, P. A.; Janssen, R. A. J.; Hummelen, J. C.; Brabec, C. J.; Shaheen, S. E.; Sariciftci, N. S. *J. Phys. Chem. B* **2001**, *105*, 11106.
(4) Peumans, P.; Uchida, S.; Forrest, S. R. *Science* **2003**, *425*, 158.
(5) Tang, C. W. *Appl. Phys. Lett.* **1986**, *48*, 183.
(6) Halls, J. J. M. *Nature* **1995**, *376*, 498.
(7) Granström, M. *Nature* **1998**, *395*, 257.
(8) Bao, Z.; Lovinger, A. J.; Brown, J. *J. Am. Chem. Soc.* **1998**, *120*, 207.
(9) Shi, M. M.; Chen, H. Z.; Shi, Y. W.; Sun, J. Z.; Wang, M. *J. Phys. Chem. B* **2004**, *108*, 5901.
(10) Hiramoto, M.; Fujiwara, H.; Yokoyama, M. *J. Appl. Phys.* **1992**, *72*, 3781.
(11) Waldauf, C.; Schilinsky, P.; Hauch, J.; Brabec, C. J. *Thin Solid Films* **2004**, *451−452*, 503.
(12) Jin, S. D.; Guan, J. W.; Shen, Q.; Chen, W. Q. *J. Inorg. Chem.* **1993**, *9*, 1
(13) Stolarski, R.; Fiksiński K. *Dyes Pigm.* **1994**, *24*, 295.
(14) Chen, H. Z.; Xu, R. S.; Wang, M. *J. Appl. Polym. Sci.* **1998**, *69*, 2609.
(15) Cao, L.; Chen, H. Z.; Wang, M.; Sun, J. Z. *J. Phys. Chem. B* **2002**, *106*, 8971.
(16) Derouiche, H.; Bernède, J. C.; Hyver, J. L. *Dyes Pigm.* **2004**, *63*, 277.
(17) Monahan, A. R.; Brado, J. A.; Deluca, A. F. *J. Phys. Chem.* **1972**, *76*, 446.
(18) Hertmanowski, R.; Biadasz, A. *J. Mol. Struct.* **2003**, *646*, 25.
(19) Bauman, D.; Schulze, H.; Kuball, H.-G. *Liq. Cryst.* **2000**, *27*, 1357.
(20) Sariciftci, N. S.; Braun, D.; Zhang, C.; Srdanov, V. I.; Heeger, A. J.; Stucky, G.; Wudl, F. *Appl. Phys. Lett.* **1993**, 6, 62.
(21) Sylvester-Hvid, K. O.; Ratner, M. A. *J. Phys. Chem. B* **2005**, *109*, 200.